Surface protein gradients generated in sealed microchannels using spatially varying helium microplasma

Pascal Wettstein,[1] Craig Priest,[2] Sameer A. Al-Bataineh,[1] Robert D. Short,[1] Paul M. Bryant,[3] James W. Bradley,[3] Suet P. Low,[1] Luke Parkinson,[2] and Endre J. Szili[1,a)]

[1]*Mawson Institute, University of South Australia, Mawson Lakes, South Australia 5095, Australia*
[2]*Ian Wark Research Institute, University of South Australia, Mawson Lakes, South Australia 5095, Australia*
[3]*Department of Electrical Engineering and Electronics, The University of Liverpool, Brownlow Hill, Liverpool L69 3GJ, United Kingdom*

(Received 15 December 2014; accepted 11 February 2015; published online 20 February 2015)

Spatially varied surface treatment of a fluorescently labeled Bovine Serum Albumin (BSA) protein, on the walls of a closed (sealed) microchannel is achieved via a well-defined gradient in plasma intensity. The microchips comprised a microchannel positioned in-between two microelectrodes (embedded in the chip) with a variable electrode separation along the length of the channel. The channel and electrodes were 50 μm and 100 μm wide, respectively, 50 μm deep, and adjacent to the channel for a length of 18 mm. The electrode separation distance was varied linearly from 50 μm at one end of the channel to a maximum distance of 150, 300, 500, or 1000 μm to generate a gradient in helium plasma intensity. Plasma ignition was achieved at a helium flow rate of 2.5 ml/min, 8.5 $kV_{pk\text{-}pk}$, and 10 kHz. It is shown that the plasma intensity decreases with increasing electrode separation and is directly related to the residual amount of BSA left after the treatment. The plasma intensity and surface protein gradient, for the different electrode gradients studied, collapse onto master curves when plotted against electrode separation. This precise spatial control is expected to enable the surface protein gradient to be tuned for a range of applications, including high-throughput screening and cell-biomolecule-biomaterial interactions. © *2015 AIP Publishing LLC*.
[http://dx.doi.org/10.1063/1.4913367]

INTRODUCTION

Microfluidics and the lab-on-a-chip concept have evolved remarkably from small groups of researchers using custom in-house "lab-on-a-chip" devices to complex, commercially available products for industrial and clinical applications.[1–5] The intense interest in developing miniaturized fluidic technologies has, for the most part, been driven by the need for a step-change in efficiency, precision, mobility, and cost for analytical chemistry and biomedicine. Increasingly, devices that meet these challenges are being applied; however, a critical factor in developing highly functional devices is the ability to reproducibly achieve robust and spatially controlled surface modification within the tiny environment of the microchannel, which is addressed in this paper.

Despite the many advances in device design and fabrication using techniques initially developed for the electronics industry,[6] several hurdles must be overcome before microfluidic technologies are more fully embraced by the healthcare industry, clinicians, and researchers. Complex microchannel designs,[7] miniaturized pumping,[8] and fluid mixing systems[9] and the use

a)E-mail: endre.szili@unisa.edu.au

of polymeric materials such as poly(dimethylsiloxane) (PDMS) have enabled microchips to be fabricated by quick and low cost methods.[10–12] However, microchips fabricated from polymeric or glass materials typically exhibit a homogeneous surface chemistry without biological functionality, and therefore are incompatible for many applications involving the use of biological cells and proteins.[13]

Adding functionality to microchips can be achieved by patterning surface chemistries on the walls of the channels of "open" microchips prior to bonding[14,15] or *in situ* through solution based methods.[16,17] Alternatively, plasma technology can be used to modify the walls of channels in bonded chips with precise control over the spatial distribution and nature of the chemistry.[18–21] The method is dry (solvent-less) making it environmentally low-impact and straight-forward. Recently, we developed a fast and reliable plasma treatment for micro-scale localized plasma treatment within bonded microchannels.[22] Structured electrode channels, i.e., ''injected'' gallium electrodes, were used to generate small regions of high electric field-strength along a bonded microchannel which, in turn, confined a plasma for targeted surface treatment. Pattern features exhibiting different chemical and biological functionalities were generated inside 50 μm $\times$ 30 μm cross-section channels over channel lengths smaller than 100 μm.[22–24]

Adding homogeneous or patterned surface functionality inside confined environments may be useful for many sensing and screening applications; however, these surfaces do not closely mimic the natural biological environment. Physiological and pathological processes are often driven by gradients of biological signals and a number of studies have shown that disaggregated individual cells sense and respond to gradients of properties on a solid material such as a slide or a tissue culture well.[25–33] Numerous physiological processes such as tissue development and diseases are also driven by gradients of biological signals.[34–38] Chemical gradients drive processes such as immune response, neovascularization, and stem cell differentiation. Chemotaxis by protein gradients increases cell motility and metastasis in cancer cell lines and promotes angiogenesis.[39–41]

A number of researchers have used microchips to generate concentration gradients in solution, making use of microfluidic networks,[42] diffusion,[43] or surface features.[44] However, there are considerably fewer reports on the development of immobilized gradients in microchips. Dertinger *et al.* immobilized a laminin gradient on a poly-L-lysine layer with the aid of a complex network of channels to study axonal growth.[27] Noor and Krull[45] used a glass–PDMS hybrid chip to generate gradients of immobilized oligonucleotide probes. The glass slide was coated with covalently immobilized aldehyde groups and the amine terminated probes were delivered by electrokinetic pumping to generate a density gradient.[45]

In this paper, we investigate the feasibility of using plasma intensity gradients to spatially control surface protein gradients along the walls of a microchannel (Fig. 1). We used fluorescein conjugated Bovine Serum Albumin (BSA) simply to demonstrate the method. Previously, we have passivated microchannels with BSA layers to block protein and cell attachment; the application of localized microplasma treatment partially removes and modifies the BSA enabling the subsequent attachment of proteins and cells to the modified regions.[23,24] Here, we show that the intensity and length of plasma gradients within enclosed microchannels can be directly related to the surface gradient of the immobilized BSA, permitting spatial control over the surface protein gradient, including in the form of smooth gradients. The plasma intensity and surface protein gradient are correlated, with both collapsing onto a master curve when plotted against electrode separation. The latter will prove useful in a variety of applications that require exceptional control over chemical or biological surface gradients in confined environments.

EXPERIMENT

Microchip fabrication

Microchips, consisting of a PDMS section with patterned microchannels and a flat glass plate, were fabricated using PDMS (Sylgard 184, Dow Corning, USA) and microscope slides. A 50 μm SU8 negative photoresist was spin-coated (Suess Delta 80, 3000 rpm) onto Si wafers

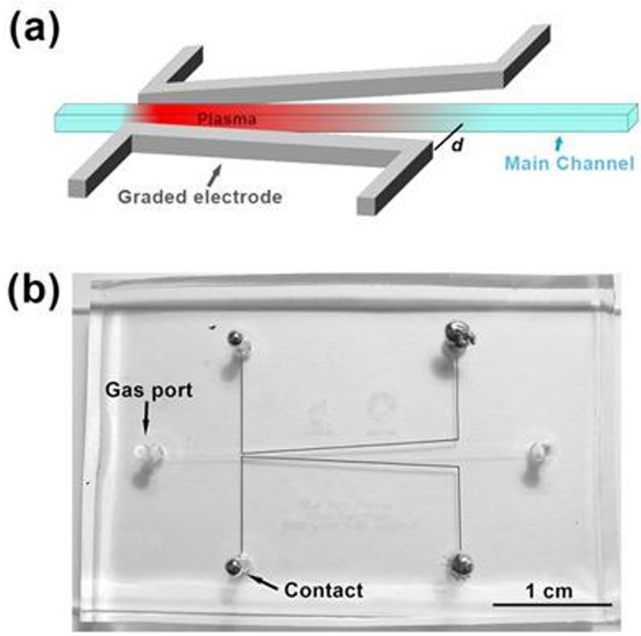

FIG. 1. Design of the microchip used to generate plasma intensity gradients in bonded microchannels. (a) Schematic showing the arrangement of the electrodes as well as the distance d, which was varied to obtain different gradients of electrode–-channel distances. (b) Glass–PDMS hybrid chip with graded gallium electrodes, $d = 1000\,\mu$m.

(50 mm dia., [100], Si-Mat, Germany), baked (4 min at 65 °C and 20 min at 95 °C), exposed (EVG620 Mask Aligner, 250 mJ cm^{-2}) and post-exposure baked (1 min at 65 °C and 4 min at 90 °C). After developing the microchannel structures, it was hard baked (ramping profile 100 °C–200 °C–100 °C) and silanized at 80 °C under vacuum ($\sim 10^{-2}$ Torr, 20 min) using hexamethyldisilane (HMDS). PDMS was cured on the master for 2 h at 65 °C. The gas and gallium inlets were created using a biopsy punch (1.5 mm, Kai Medical, Germany) after removal of the PDMS structure.

The microscope slides were rinsed with acetone and isopropanol, dried under nitrogen, plasma cleaned (oxygen, 5 min, Harrick Plasma Cleaner), and chemically bonded to the PDMS structure. The PDMS surface was activated via oxygen plasma treatment (15 s, Harrick Plasma Cleaner) before compressing the PDMS and glass sections together for 30 min in ambient atmosphere. Alongside the 50 μm wide main channel with length of 18 mm, two electrode guides were included in the photomask (JD Photo-Tools, UK). These guides were graded, i.e., the distance between the electrode guide and the main channel was constant (50 μm) at one end of the channel and varied on the other (d in Fig. 1(a)). The designs are $d = 150$, 300, 500, and 1000 μm and, as reference, a non-graded channel design ($d = 50\,\mu$m). The width of electrode guides is 100 μm and the depth is determined by the thickness of the photoresist layer (50 μm). The injection of the gallium electrodes is described elsewhere.[22] Briefly, gallium is heated to 50 °C, drawn into an ethylene vinyl acetate microbore tubing (Cole Parmer) with a 1 ml syringe and injected into the guide. The electrodes are solidified by adding a seed crystal to a droplet of gallium protruding from the inlet.

Plasma operation

A custom-built power supply to generate the plasma is described elsewhere.[46] Briefly, a step-up transformer capable of delivering up to 10 kV_{pk-pk} and 40 mA_{pk-pk} with a frequency range of 5–20 kHz (Southern Electronic Services), an audio amplifier (AMPRO XA1400), and an oscillator (Agilent Technologies DS06034A) was used to generate the necessary sinusoidal AC excitation to generate the plasma. The microchips were assembled into a custom-built holder to enable power to be safely delivered to the microfluidic chips via coaxially shielded

cables. Helium (He, BOC high purity grade) gas was fed into the central channel via EVA microbore tubing (Cole Parmer) connecting the gas inlet of the central channel to a mass flow controller (Apex E-series, 0–5 sccm flow range), used to regulate the gas flow. The channel was pre-flushed with 2.5 ml/min of He for 15 min. Plasma, in the central channel, was ignited with a He flow rate of 2.5 ml/min, at 8.5 $kV_{pk\text{-}pk}$ and 10 kHz.

The visible plasma discharge was imaged with a Nikon DXM1200C digital camera mounted on a Nikon Inverted Microscope TE-2000. In order to image the whole channel, 10–12 images had to be taken on a manual stage, which were then manually stitched using Photoshop. Intensity profiles of the plasmas were measured using NIS Elements 3.2 (Nikon).

Generation of surface protein gradients

A 100 μg/ml solution of fluorescein conjugated BSA (Invitrogen) in phosphate buffered saline (PBS, Sigma Aldrich) was injected into the central channel and left to incubate at 25 °C for 12 h. The channel was washed by flushing with PBS for 2 min followed by drying with 2.5 ml/min He for 15 min. The BSA modified channel was subsequently exposed to the plasma for 5 s as described above. We repeated the procedure for a few of the electrode designs to confirm that the procedure was reproducible.

Imaging of surface protein gradients

Fluorescein conjugated BSA was imaged inside the microchannels with a Nikon Inverted Microscope TE-2000 through a 4× objective fitted with a Nikon GFP HQ filter (excitation 455–485 nm, dichroic mirror 495 nm, and barrier filter 500–545 nm). In order to image the whole channel, multiple images were stitched together as described above. After plasma treatment, the channels were re-imaged and an intensity profile of the fluorescence in the treated channel was obtained using NIS Elements 3.2.

Surface characterisation of surface protein gradients

These experiments were performed using separable microchips (that were not chemically bonded) and a custom-built compression fixture. The reaction channel was functionalized with BSA and plasma treated as described above. The PDMS and glass sections were then separated. Only the glass section was inspected due to incompatibilities with mounting the PDMS inside the surface analysis instruments.

For time-of-flight secondary ionization mass spectrometry (ToF-SIMS) analysis, the glass section was cut into three sections representing the main channel treated with the plasma at the two extremities and middle region of the electrode gradients. ToF-SIMS measurements were performed using a Physical Electronics Inc., PHI TRIFT V nanoToF instrument equipped with a pulsed liquid metal $^{79}Au^{+}$ primary ion gun (LMIG), operating at 30 kV. Surface analyses were performed using "bunched" Au_1 beam settings to optimize mass resolution. Spectra were collected in positive SIMS mode, typically using 100 × 100 μm raster areas. Experiments were performed under a vacuum of $\leq 3.8 \times 10^{-8}$ Torr and in the static mode to minimize possible effects arising from sample damage.

For scanning electron microscopy (SEM) analysis, the entire glass section was mounted into the instrument for inspection. SEM was performed on a FEI Quanta 450 operating at 10 keV at a working distance of 10 mm. Elemental composition of the surface was probed with an energy dispersive X-ray (EDX) spectroscope equipped with a SDD EDS detector coupled to the SEM. Measurements were performed in triplicate.

RESULTS AND DISCUSSION

Varying the plasma intensity along the microchannel

The design of the microchip is schematically depicted in Fig. 1. By varying the electrode separation along the channel, an electric field gradient is generated when the electrical potential

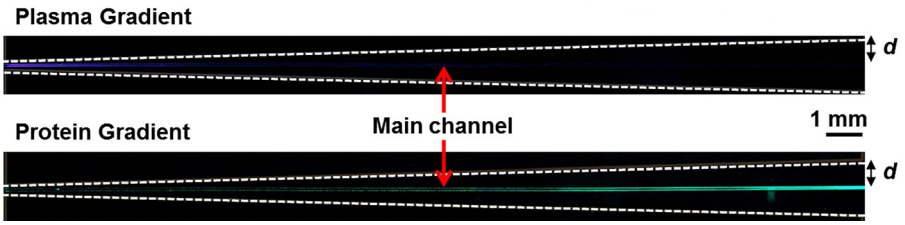

FIG. 2. Plasma intensity gradient generates a protein gradient ($d = 500\,\mu$m) inside a bonded microchip. A gradient of plasma intensity inside the bonded microchannel is shown in the top optical micrograph and the corresponding protein gradient of BSA is shown in the fluorescence micrograph below. The white dashed lines in the figures represent the position of the electrodes.

is applied. An example of the plasma intensity gradient is shown in Fig. 2 for electrode design $d = 500\,\mu$m. The plasma intensity (indicated by the blue color) is observed to decrease as the electrode separation increased from left to right along the length of the channel. Results for the four different plasma intensity gradients in electrode separation are plotted in Fig. 3, along with the reference data (i.e., no gradient) which shows no significant change in plasma intensity over the full length of the channel. Clearly, for variable electrode separations, the plasma intensity decreased more sharply with increasing d, as one might expect. In each case, the plasma intensity decays as a function of the channel position, Fig. 3(a), and, for large values of d, the

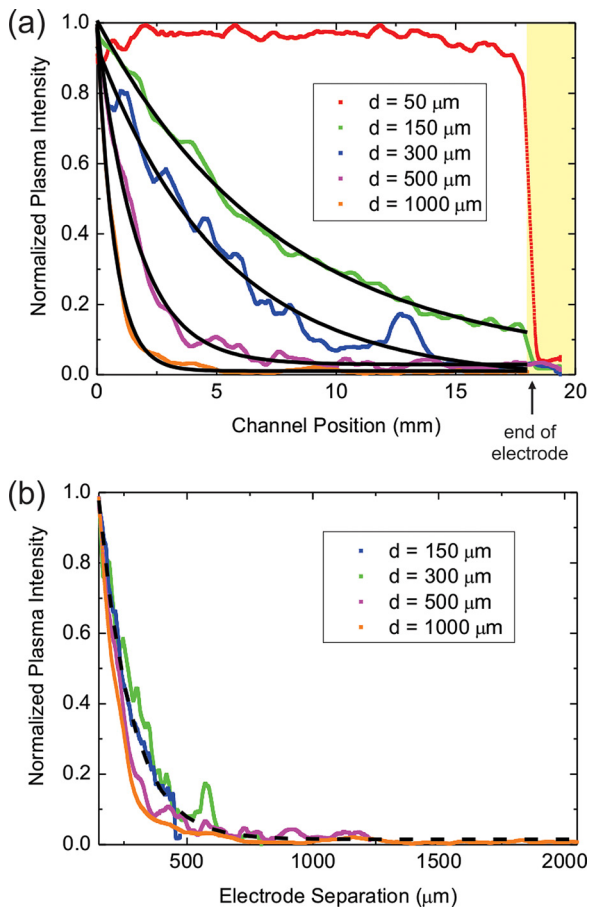

FIG. 3. Normalized plasma emission intensity profiles for plasma intensity gradients generated in microchannels. The channel position is measured from the end of the channel with the smallest electrode separation. (a) Experimental results for $d = 50\,\mu$m (reference; no gradient), 150 μm, 300 μm, 500 μm, and 1000 μm, with best fits are shown. (b) Collapse of experimental results for the plasma intensity gradients plotted against electrode separation.

plasma intensity reduces to zero prior to the end of the channel. The step-like fluctuations in the curves are due to stitching of images that were used to follow the intensity along the entire channel. Channel position is linearly related to the electrode separation for each gradient studied and, therefore, it is possible to reconsider the results in terms of electrode separation alone. Fig. 3(b) shows a plot of the plasma intensity against the electrode separation for the four gradients studied. These results collapse onto a single master curve, demonstrating that the plasma intensity and gradient of intensity can be precisely tuned by controlling electrode separation alone. The decay of the plasma intensity with electrode separation can be explained by considering that the electric field decreases along the channel due to the increased separation of the electrodes. Generally, lower electric fields reduce the energy gained by electrons being accelerated. Consequently, the ability for electrons to ionize or excite atoms is decreased leading to lower electron densities along the channel and reduced light emission.

Knowing the governing relationship between plasma intensity and electrode separation provides a good handle for studying the effect of the plasma on the microchannel surface chemistry. The following subsections ("Surface protein gradients" and "Surface analysis of BSA gradients") will discuss how the plasma gradient is transferred to the channel walls as a protein gradient when the channel is pre-treated with BSA.

Surface protein gradients

The efficacy of using plasma with an emission intensity gradient to generate a surface protein gradient within a bonded microchannel was tested. Prior to treatment, the fluorescein fluorescence intensity was homogenous along the channel, corresponding to an even coating of the BSA onto the channel walls (Fig. 4(a)). After plasma treatment, a gradient of fluorescein fluorescence intensity can be seen along the microchannel, as shown for $d = 500\,\mu$m in Fig. 2. Assuming that the fluorescence intensity can be related to the amount of protein on the channel walls, these results demonstrate that a plasma intensity gradient can be used to precisely generate protein gradients in confined geometries, including microchannels. We have prepared these protein gradients in both glass and poly(dimethylsiloxane) (PDMS) microchannels. Similar fluorescence intensity (protein) gradients were produced on both PDMS and glass surfaces by the plasma treatment (data not shown). The polarity of the transfer of plasma intensity gradient to the protein layer is positive: the plasma removes and/or chemically modifies the BSA in exposed regions, with the efficacy of the process greater for higher plasma intensities.

Fig. 4(a) shows the fluorescence intensity of fluorescein conjugated BSA measured along the length of the microchannel after treatment. The fluorescence intensity is very low for the straight electrode design ($d = 50\,\mu$m) and the smallest gradient design of $d = 150\,\mu$m, indicating that nearly all of the protein was removed by the plasma treatment in these microchips. A gradient fluorescence signal in the channel is observed for electrode designs with $d = 300$, 500, and $1000\,\mu$m. The channel position is measured from the end of the electrodes with the smallest electrode-channel separation ($50\,\mu$m), so that the higher plasma intensity is to the left of Fig. 4(a), where the fluorescence intensity is near zero in all cases. Less BSA was removed by the plasma treatment downstream where the plasma intensity gradually diminished. Past the end of the electrodes, indicated by the yellow shading in Fig. 4(a), the fluorescence intensity increases towards the maximum (untreated) intensity, however the transition is not very sharp. In fact, the surface treatment affects the channel surface up to several millimeters downstream of the electrodes, which we attribute to transport of plasma species downstream by the gas flow. The data presented in this paper were obtained by the plasma treatment where helium flowed from the narrowest electrode separation end to the widest separation end (i.e., from left to right in Fig. 2). But in one set of experiments, the direction of helium flow was reversed.[47] This resulted in a lower amount of BSA removal and a steeper protein gradient. We attribute this observation to the gas flow influencing the migration of the plasma reactive species outside of the plasma zone. With the gas flowing left-to-right, a higher amount of BSA may have been removed due to the plasma reactive species migrating downstream resulting in higher amount of BSA removal/modification.

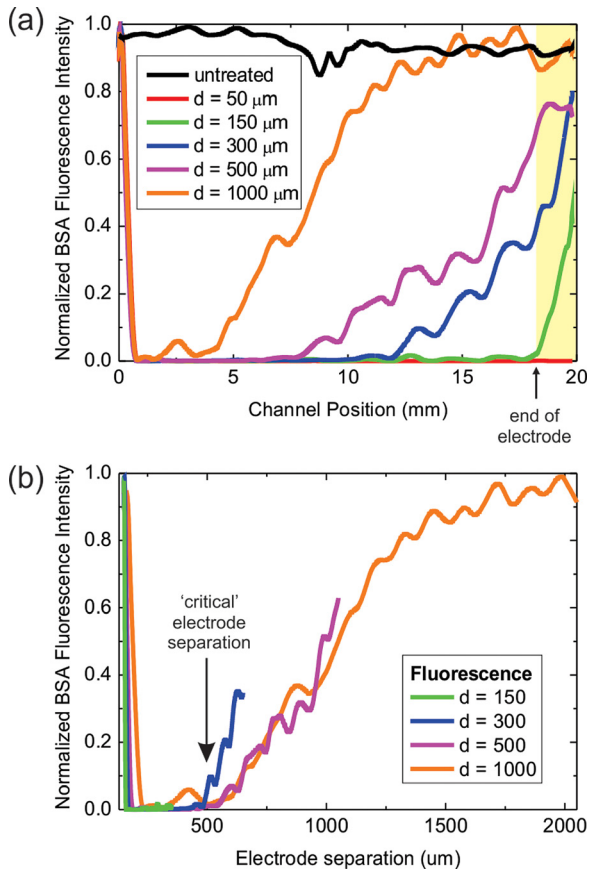

FIG. 4. Normalized fluorescence intensity profiles for fluorescein conjugated BSA along channels that were treated with plasma intensity gradients. The channel position is measured from the end of the channel with the smallest electrode separation. (a) Experimental results plotted versus channel position for $d = 50\,\mu$m (reference; no plasma gradient), $150\,\mu$m, $300\,\mu$m, $500\,\mu$m, and $1000\,\mu$m. (b) Collapse of the experimental results plotted versus electrode separation showing a "critical" electrode separation; negligible fluorescence signal was detected prior to this critical separation for all electrode configurations studied.

Fig. 4(b) shows the fluorescence intensity (of fluorescein conjugated BSA) after plasma treatment plotted against the electrode separation. The fluorescence intensity results collapse reasonably well when plotted in this way, demonstrating that electrode separation governs the

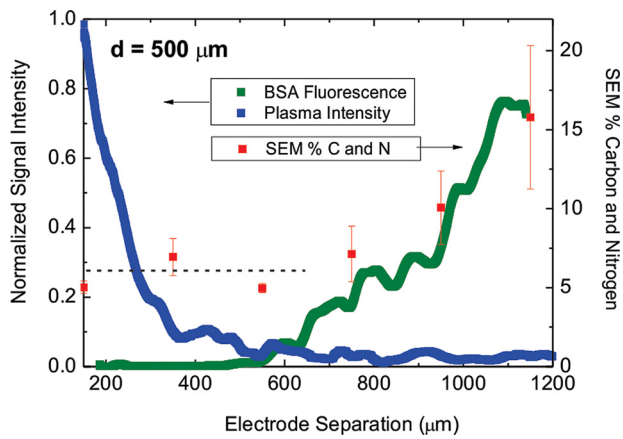

FIG. 5. Comparison of crossover between plasma intensity and BSA fluorescence signals at the critical electrode separation for $d = 500\,\mu$m. Scanning electron microscopy EDX measurements of carbon and nitrogen show good agreement with the BSA fluorescence intensity, where the baseline is estimated between 5 and 7 at. % carbon and nitrogen.

plasma intensity gradient as well as the resulting protein gradient. Fig. 4(b) also reveals a "critical" electrode separation below which plasma treatment using our chosen parameters (i.e., He flow rate of 2.5 ml/min, 8.5 $kV_{pk\text{-}pk}$, and 10 kHz) quenches the fluorescence signal completely. In these experiments, the critical electrode separation was estimated to be 500 μm. Fig. 5 shows the cross-over of the plasma intensity and fluorescence intensity profiles near the critical electrode separation. The correlation between the two profiles is very clear; however it should be noted that the BSA layer appears to be affected at high electrode separations despite the plasma intensity being nearly zero. It is not possible to differentiate between the impact of plasma species generated locally and those transported downstream, but, as discussed above, gas flow direction does impact the protein intensity profile.

Surface analysis of BSA gradients

In order to characterize the surface chemistry of the BSA gradients fabricated in the microchips, we used the custom-built compression fixture again that allowed us to safely operate the plasma in the chips and separate the halves for inspection. Only glass plates were characterized due to difficulties associated with mounting the PDMS material into the sample analysis chambers. Although we did not characterize the chemistry of the PDMS microchannels in this study, we appreciate that the surface chemistry would be different between the permanently bonded microchips (where PDMS was treated an O_2 plasma for chemical-bonding) and the compression-bonded chips. However, this chemistry difference should not be permanent due to molecular reorientation of the modified surface functional groups; moreover, the surfaces of the PDMS microchannels are subsequently completed covered with BSA prior to plasma treatment. In addition, the difference in the surface chemistry of the materials A microchip with electrode design $d = 500\ \mu$m, was analysed.

For ToF-SIMS analysis, the glass slide was cut into three sections at 0–5 (a), 8–13 (b), and 13–18 (c) mm along the channel from the narrow to wider electrode separation end. Fig. 6

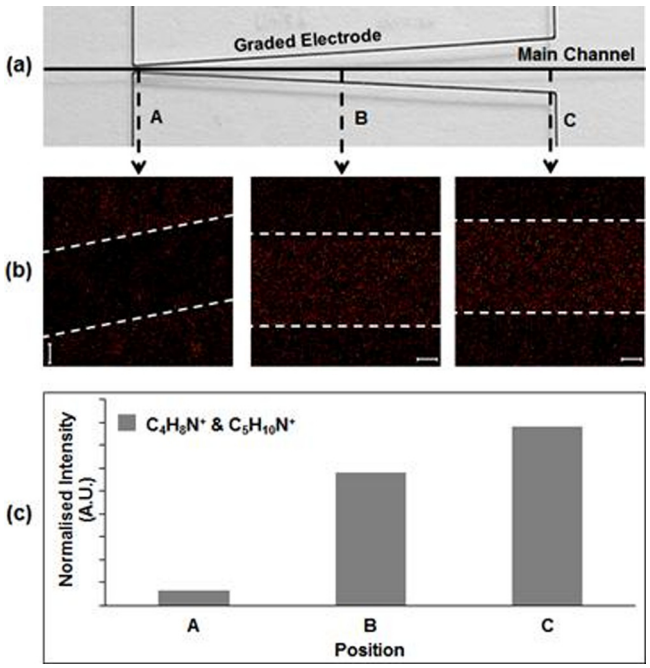

FIG. 6. ToF-SIMS analysis of the BSA-coated microchannel after plasma intensity gradient treatment for 5 s. (a) A photograph, of the glass–PDMS hybrid chip with graded gallium electrodes, $d = 500\ \mu$m, highlighting the three regions (A, B, and C) that were analysed by ToF-SIMS. (b) Total ToF-SIMS images (100 μm × 100 μm) of the BSA-associated positive fragments ($C_4H_8N^+$, 70.070 amu and $C_5H_{10}N^+$, 84.080 amu); and (c) a column chart showing the total intensity of $C_4H_8N^+$ and $C_5H_{10}N^+$ normalized to the total counts in each spectrum acquired from the selected regions alongside the microchannel. This data confirm that a surface gradient of BSA was produced in the microchannel.

shows positive ToF-SIMS images of the total intensity of two fragment ions ($C_4H_8N^+$, 70.070 amu and $C_5H_{10}N^+$, 84.080 amu) associated with the BSA. There is little difference in intensity between the images collected from regions B and C, whereas the difference in intensity is very clear when compared to the ToF-SIMS image collected from region A. To illustrate the differences between these images further, region of interest (ROI) mass spectra were collected from each image. The combined intensities of $C_4H_8N^+$ and $C_5H_{10}N^+$ were normalized to the total counts in each spectrum and plotted in a column chart (Fig. 6(c)). This shows that there is a BSA gradient in the main channel.

SEM inspection provided further evidence for the generation of surface protein gradients by the plasma intensity gradient treatment procedure. The glass plate with the microchannel feature was inserted into the SEM chamber for analysis. Due to significant overlap in both peaks, the combination of both the carbon and nitrogen peaks were utilized as markers for the presence of the protein—both are abundant in the chemical composition of proteins but not on the glass. Fig. 5 shows that the carbon/nitrogen signal was low (5–6 at. %) in the region of the channel treated with the plasma at the high intensity end (below approximately 500 μm electrode separation). As the plasma intensity decreased beyond the critical electrode separation, the concentration of carbon/nitrogen increased significantly and follows the trend of the fluorescence intensity. Together with the ToF-SIMS results, these SEM results demonstrate that the fluorescence intensity gradients (for fluorescein conjugated BSA) observed in the plasma treated channels, is not a result of the quenching of the fluorophore. Rather, it corresponds to removal and modification of BSA from the channel walls, commensurate with the applied plasma intensity gradients. Previously, we found that this modification enables subsequent attachment of proteins and cells to regions of the BSA layers that were modified by the microplasma treatment.[23,24]

SUMMARY AND OUTLOOK

We investigated a plasma intensity gradient treatment approach to fabricate surface gradients of protein in bonded microchannels. First, we show that microchips with graded electrodes adjacent to the main channel can be used to generate plasmas with gradient intensities along the length of the microchannel and that the slope and length of the plasma intensity gradient is strongly dependent on the slope of the electrodes. Second, these plasmas were used to treat bonded microchannels that were pre-functionalised with BSA protein. The treatment resulted in the removal and modification of BSA in a continuous gradient fashion with a higher amount of BSA removed at the narrower electrode separation end compared to the wider end.

The intensity of the plasma and by inference the density of the energetic and reactive species, e.g., ions, neutrals, photons, excited metastables, and other species, was controlled by varying the electrode separation distance along the microchannel. This resulted in the removal of BSA from the microchannel walls in a gradient fashion. Since BSA is a relatively cheap, readily available and a widely employed "blocking agent",[48] we believe our approach is a viable option in the fabrication or generation of protein, antibody, enzyme, and cell gradients in microchips for use in bioassays. We have previously demonstrated the efficacy of using plasma to activate BSA passivated "open" surfaces and walls of enclosed micochannels for subsequent binding of proteins, antibodies, enzymes, and cells, and so this was not repeated here.[24] Instead, we have studied the generation of plasma intensity gradients inside bonded microchannels and their use in generating BSA gradients. This approach could be adapted in the future for tailoring the adhesivity of microchannel surfaces passivated with other chemistries, e.g., poly(ethylene)glycols;[49] or alternatively be used for other applications such as activating microchannel surfaces for fluid control. Further study of the plasma environment through diagnosis of the plasma will enable us to understand and tailor the plasma to achieve reliable use of plasma inside confined capillary spaces, and therefore, deliver enhanced process control (e.g., for introducing new chemical or biomolecule functionalities into microchips) and address future challenging applications of this technology.

ACKNOWLEDGMENTS

The microfluidic devices were fabricated at the South Australian node of the Australian National Fabrication Facility (ANFF-SA). We would like to thank the ANFF-SA staff for the use of state-of-the-art facilities and their technical assistance. Part of this work was supported by the ANFF-SA start-up award. We thank Doug Veale (Cantech) for the design and construction of the power supply and the microchip holder.

[1]H. Craighead, Nature **442**, 387 (2006).
[2]A. J. deMello, Nature **442**, 394 (2006).
[3]J. El-Ali, P. K. Sorger, and K. F. Jensen, Nature **442**, 403 (2006).
[4]J. Tian, H. Gong, N. Sheng, X. Zhou, E. Gulari, X. Gao, and G. Church, Nature **432**, 1050 (2004).
[5]G. M. Whitesides, Nature **442**, 368 (2006).
[6]A. Manz, J. C. Fettinger, E. Verpoorte, H. Lüdi, H. M. Widmer, and D. J. Harrison, TrAC, Trends Anal. Chem. **10**, 144 (1991).
[7]M. K. S. Verma, A. Majumder, and A. Ghatak, Langmuir **22**, 10291 (2006).
[8]K. Handique, D. T. Burke, C. H. Mastrangelo, and M. A. Burns, Anal. Chem. **73**, 1831 (2001).
[9]A. P. Sudarsan and V. M. Ugaz, Lab Chip **6**, 74 (2006).
[10]D. Qin, Y. Xia, and G. M. Whitesides, Adv. Mater. **8**, 917 (1996).
[11]D. C. Duffy, J. C. McDonald, O. J. A. Schueller, and G. M. Whitesides, Anal. Chem. **70**, 4974 (1998).
[12]D. J. Beebe, J. S. Moore, Q. Yu, R. H. Liu, M. L. Kraft, B. H. Jo, and C. Devadoss, Proc. Natl. Acad. Sci. U.S.A. **97**, 13488 (2000).
[13]J. Zhou, N. H. Voelcker, and A. V. Ellis, Biomicrofluidics **4**, 046504 (2010).
[14]M. Salim, G. Mishra, G. J. S. Fowler, B. O'Sullivan, P. C. Wright, and S. L. McArthur, Lab Chip **7**, 523 (2007).
[15]M. Salim, P. C. Wright, and S. L. McArthur, Electrophoresis **30**, 1877 (2009).
[16]H. Kaji, M. Hashimoto, and M. Nishizawa, Anal. Chem. **78**, 5469 (2006).
[17]B. Zhao, J. S. Moore, and D. J. Beebe, Science **291**, 1023 (2001).
[18]J. K. Evju, P. B. Howell, L. E. Locascio, M. J. Tarlov, and J. J. Hickman, Appl. Phys. Lett. **84**, 1668 (2004).
[19]C. P. Klages, C. Berger, M. Eichler, and M. Thomas, Contrib. Plasma Phys. **47**, 49 (2007).
[20]C.-P. Klages, A. Hinze, K. Lachmann, C. Berger, J. Borris, M. Eichler, M. von Hausen, A. Zänker, and M. Thomas, Plasma Processes Polym. **4**, 208 (2007).
[21]S. Thorslund and F. Nikolajeff, J. Micromech. Microeng. **17**, N16 (2007).
[22]C. Priest, P. J. Gruner, E. J. Szili, S. A. Al-Bataineh, J. W. Bradley, J. Ralston, D. A. Steele, and R. D. Short, Lab Chip **11**, 541 (2011).
[23]E. J. Szili, S. A. Al-Bataineh, C. Priest, P. J. Gruner, P. Ruschitzka, J. W. Bradley, J. Ralston, D. A. Steele, and R. D. Short, Proc. SPIE **8204**, 82042J (2011).
[24]E. J. Szili, S. A. Al-Bataineh, P. Ruschitzka, G. Desmet, C. Priest, H. J. Griesser, N. H. Voelcker, F. J. Harding, D. A. Steele, and R. D. Short, RSC Adv. **2**, 12007 (2012).
[25]G. Maheshwari, G. Brown, D. A. Lauffenburger, A. Wells, and L. G. Griffith, J. Cell Sci. **113**, 1677 (2000); available at http://jcs.biologists.org/content/113/10/1677.abstract.
[26]S. T. Plummer, Q. Wang, P. W. Bohn, R. Stockton, and M. A. Schwartz, Langmuir **19**, 7528 (2003).
[27]S. K. W. Dertinger, X. Jiang, Z. Li, V. N. Murthy, and G. M. Whitesides, Proc. Natl. Acad. Sci. U.S.A. **99**, 12542 (2002).
[28]M. Zelzer, R. Majani, J. W. Bradley, F. R. A. J. Rose, M. C. Davies, and M. R. Alexander, Biomaterials **29**, 172 (2008).
[29]N. Wells, M. A. Baxter, J. E. Turnbull, P. Murray, D. Edgar, K. L. Parry, D. A. Steele, and R. D. Short, Biomaterials **30**, 1066 (2009).
[30]A. Michelmore, L. Clements, D. A. Steele, N. H. Voelcker, and E. J. Szili, J. Nanomater. **2012**, 839053 (2012).
[31]J. Genzer and R. R. Bhat, Langmuir **24**, 2294 (2008).
[32]S. Morgenthaler, C. Zink, and N. D. Spencer, Soft Matter **4**, 419 (2008).
[33]C. E. Kang, E. J. Gemeinhart, and R. A. Gemeinhart, J. Biomed. Mater. Res. Part A **71A**, 403 (2004).
[34]D. M. Bryant and K. E. Mostov, Nat. Rev. Mol. Cell Biol. **9**, 887 (2008).
[35]J. B. Gurdon and P. Y. Bourillot, Nature **413**, 797 (2001).
[36]T. Lecuit and L. Le Goff, Nature **450**, 189 (2007).
[37]D. Rogulja and K. D. Irvine, Cell **123**, 449 (2005).
[38]A. J. Zhu and M. P. Scott, Genes Dev. **18**, 2985 (2004).
[39]S. A. Eccles, Curr. Opin. Genet. Dev. **15**, 77 (2005).
[40]T. Jin, X. Xu, and D. Hereld, Cytokine **44**, 1 (2008).
[41]W. Wang, R. Eddy, and J. Condeelis, Nat. Rev. Cancer **7**, 429 (2007).
[42]S. K. W. Dertinger, D. T. Chiu, N. L. Jeon, and G. M. Whitesides, Anal. Chem. **73**, 1240 (2001).
[43]W. Saadi, S. W. Rhee, F. Lin, B. Vahidi, B. G. Chung, and N. L. Jeon, Biomed. Microdevices **9**, 627 (2007).
[44]D. Friedrich, C. P. Please, and T. Melvin, Chem. Eng. J. **193–194**, 296 (2012).
[45]M. O. Noor and U. J. Krull, Anal. Chim. Acta **708**, 1 (2011).
[46]S. A. Al-Bataineh, E. J. Szili, A. Mishra, S.-J. Park, J. G. Eden, H. J. Griesser, N. H. Voelcker, R. D. Short, and D. A. Steele, Plasma Processes Polym. **8**, 695 (2011).
[47]See supplementary material at http://dx.doi.org/10.1063/1.4913367 for plasma intensity and protein gradients produced with reversed helium flow.
[48]Y. Xiao and S. N. Isaacs, J. Immunol. Methods **384**, 148 (2012).
[49]D. J. Menzies, B. Cowie, C. Fong, J. S. Forsythe, T. R. Gengenbach, K. M. McLean, L. Puskar, M. Textor, L. Thomsen, M. Tobin, and B. W. Muir, Langmuir **26**, 13987 (2010).